



## Interannual variability of mid-tropospheric CO<sub>2</sub> from Atmospheric Infrared Sounder

Xun Jiang,<sup>1</sup> Moustafa T. Chahine,<sup>2</sup> Edward T. Olsen,<sup>2</sup> Luke L. Chen,<sup>2</sup> and Yuk L. Yung<sup>3</sup>

Received 12 February 2010; revised 10 May 2010; accepted 21 May 2010; published 1 July 2010.

[1] Atmospheric Infrared Sounder (AIRS) offers a unique opportunity to investigate the variability of mid-tropospheric CO<sub>2</sub> over the entire globe. In this paper, we use AIRS data to examine the interannual variability of CO<sub>2</sub> and find significant correlations between AIRS mid-tropospheric CO<sub>2</sub> and large-scale atmospheric dynamics. During El Niño events, mid-tropospheric CO<sub>2</sub> over the central Pacific Ocean is enhanced whereas it is reduced over the western Pacific Ocean as a result of the change in the Walker circulation. The variation of AIRS CO<sub>2</sub> in the high latitudes of the northern hemisphere is closely related to the strength of the northern hemispheric annular mode. These results contribute to a better understanding of the influence of large-scale dynamics on tracer distributions. **Citation:** Jiang, X., M. T. Chahine, E. T. Olsen, L. L. Chen, and Y. L. Yung (2010), Interannual variability of mid-tropospheric CO<sub>2</sub> from Atmospheric Infrared Sounder, *Geophys. Res. Lett.*, 37, L13801, doi:10.1029/2010GL042823.

### 1. Introduction

[2] The increasing level of atmospheric CO<sub>2</sub> has a significant influence on global climate change [Dickinson and Cicerone, 1986]. Observations show a global trend of CO<sub>2</sub> of approximately 2 ppm/year [Keeling et al., 1995]. Superimposed upon this trend is an annual cycle resulting from the uptake and release of CO<sub>2</sub> by vegetation whose amplitude is greatest in the northern hemisphere (NH). In addition to the trend and the annual cycle, atmospheric CO<sub>2</sub> also shows interannual variability. In this paper, we will investigate the interannual variability of mid-tropospheric CO<sub>2</sub> and related it to the large-scale dynamics of the atmosphere.

[3] El Niño–Southern Oscillation (ENSO) is the most important source of large-scale climate interannual variability in the tropics. Atmospheric CO<sub>2</sub> is influenced by ENSO at the surface [Bacastow, 1976; Bacastow et al., 1980]. During El Niño (La Niña) events, the atmospheric CO<sub>2</sub> growth rate increases (decreases) at surface stations [Keeling et al., 1995; Jones et al., 2001]. The reasons are as follows.

[4] During El Niño events, the ocean is a sink for CO<sub>2</sub> [Feely et al., 1987; Inoue and Sugimura, 1992; Wong et al.,

1993; Feely et al., 1997, 2006]. Upwelling of the cold nutrient-rich water off the South American coast ceases during El Niño, causing the surface pCO<sub>2</sub> concentration to decrease along the equator [Feely et al., 1987, 1997]. Meanwhile, the tropical land becomes dryer and warmer. As a result, the gross primary productivity decreases and respiration increases over the land [Jones et al., 2001]. Thus the terrestrial biosphere becomes a greater source of CO<sub>2</sub> to the atmosphere during El Niño [Keeling et al., 1995; Francey et al., 1995]. The net effect from land and ocean is that the surface CO<sub>2</sub> growth rate increases during El Niño events. Conversely, the surface CO<sub>2</sub> growth rate decreases during La Niña events.

[5] The focus of these previous studies is on the influence of climate variability on the CO<sub>2</sub> concentration at a few stations near the surface. However, there is no previous investigation on the influence of El Niño on the mid-tropospheric CO<sub>2</sub> at a global scale. In this paper, we analyze the influence of ENSO on the mid-tropospheric CO<sub>2</sub> retrieved by the Atmospheric Infrared Sounder (AIRS). This global dataset provides new insight on how ENSO influences the interannual variability of CO<sub>2</sub> in the middle troposphere and contributes to our understanding of the vertical transport of tracers between the surface and the mid-troposphere.

[6] The global coverage of AIRS CO<sub>2</sub> retrievals also allows us to investigate the influence of large-scale dynamics on the CO<sub>2</sub> concentration in the polar region. Northern hemispheric polar region has profound significance for climate, for the largest changes are expected in Arctic due to climate change. Current general circulation models (GCMs) do not perform well in the polar region, especially in simulating the exchange between the stratosphere and troposphere in that region [Meloan et al., 2003]. Therefore, observations are essential for improving our understanding of the large-scale dynamics in the polar region. However, most observations and measurements in the polar region suffer from limited coverage both in time and space. The global distribution of CO<sub>2</sub> retrieved from AIRS offers a unique opportunity for studying the large-scale dynamics in the polar region.

[7] The annular modes are the most important source of interannual variability in the polar region [Thompson and Wallace, 1998]. Jiang et al. [2008a, 2008b] applied principal component analysis to the extratropical total column ozone from the combined Merged Ozone Data product and the European Center for Medium-Range Weather Forecasts assimilated ozone from Jan 1979 to Aug 2002. In each hemisphere, the first leading mode is nearly zonally symmetric and is related to the annular mode. When the polar vortex is stronger (positive phase of the annular mode), there is less ozone transported to the polar region due to a weaker Brewer–Dobson circulation. Similar results in extratropical

<sup>1</sup>Department of Earth and Atmospheric Sciences, University of Houston, Houston, Texas, USA.

<sup>2</sup>Science Division, Jet Propulsion Laboratory, California Institute of Technology, Pasadena, California, USA.

<sup>3</sup>Division of Geological and Planetary Sciences, California Institute of Technology, Pasadena, California, USA.

column ozone are found in the Goddard Earth Observation System Chemistry–Climate Model (GEOS–CCM) [Jiang *et al.*, 2008a, 2008b]. Since there is no chemical destruction of CO<sub>2</sub>, in contrast to O<sub>3</sub>, CO<sub>2</sub> is a better tracer for investigating the large-scale dynamics in the polar region. In this paper, we will examine the influence of the northern hemispheric annular mode on AIRS mid-tropospheric CO<sub>2</sub>.

## 2. Data

[8] AIRS is a cross-track scanning grating spectrometer with 2378 channels from 3.7 to 15.4  $\mu\text{m}$  with a 13.5 km field of view at nadir [Aumann *et al.*, 2003]. Chahine *et al.* [2005] found that the range 690–725  $\text{cm}^{-1}$  is best for selecting the main channel set to retrieve the mid-tropospheric CO<sub>2</sub> mixing ratio. The mixing ratios of mid-tropospheric CO<sub>2</sub> are retrieved using the Vanish Partial Derivative Method (VPD) [Chahine *et al.*, 2005, 2008]. The weighting function of AIRS mid-tropospheric CO<sub>2</sub> channels peaks between 500 hPa to 300 hPa. AIRS mid-tropospheric CO<sub>2</sub> is retrieved globally in the middle troposphere day and night under clear and cloudy conditions. We regridded AIRS CO<sub>2</sub> retrievals to  $2^\circ \times 4^\circ$  (latitude by longitude). AIRS mid-tropospheric CO<sub>2</sub> are available from September 2002 to February 2010. Validation by comparison to *in situ* aircraft measurements and retrievals by land-based upward looking Fourier Transform Interferometers demonstrates that AIRS CO<sub>2</sub> is accurate to 1–2 ppm between latitudes 30°S and 80°N [Chahine *et al.*, 2005, 2008]. The mid-tropospheric CO<sub>2</sub> retrieved via the VPD method captures the correct seasonal cycle and trend compared with those from Comprehensive Observation Network for Trace gases by AirLiner (CONTRAIL) [Chahine *et al.*, 2005].

## 3. Results and Discussions

[9] In order to investigate the interannual variability of CO<sub>2</sub>, we first remove a linear trend from the data at each latitude band. The annual cycle, determined by evaluating the mean value for each month, will be removed from the detrended CO<sub>2</sub>. The interannual variability of CO<sub>2</sub> in the tropics and the polar region will be discussed in sections 3.1 and 3.2, respectively.

### 3.1. Interannual Variability of Tropical AIRS CO<sub>2</sub>

[10] We will explore the interannual variability of tropical CO<sub>2</sub> and the influence of ENSO on CO<sub>2</sub> in this section. ENSO is the most dominant source of large-scale climate variability in the tropics. The Southern Oscillation Index (SOI) is defined as the monthly mean sea level pressure difference between Tahiti and Darwin. Negative (positive) SOI index corresponds to an El Niño (La Niña) event. In this paper, we choose El Niño (La Niña) events when the SOI index is one standard deviation below (above) the mean value. There are 11 El Niño months whose indices are one standard deviation below the mean value of SOI. There are 17 La Niña months whose SOI indices are one standard deviation above the mean value of SOI. We calculate mean values of AIRS detrended and deseasonalized CO<sub>2</sub> for 11 El Niño months and for 17 La Niña months. Figures 1a and 1b show the spatial patterns of the detrended and deseasonalized AIRS CO<sub>2</sub> for El Niño and La Niña events, respectively.

[11] During an El Niño event (Negative SOI index), warm sea surface temperature (SST) anomalies appear in the central and eastern Pacific and cold anomalies appear in the western Pacific, and the convection will move eastward to the central Pacific [Gage and Reid, 1987]. As a result, convection in the central Pacific brings surface CO<sub>2</sub> into middle troposphere. In Figure 1a, AIRS detrended and deseasonalized CO<sub>2</sub> data for 11 El Niño months indicate that surface layer CO<sub>2</sub> has been lifted into the middle troposphere over the central Pacific region during the El Niño event. Low concentration of mid-tropospheric CO<sub>2</sub> is seen in the western Pacific Ocean, associated with the sinking motion of the Walker Circulation.

[12] In contrast, during a La Niña event (Positive SOI index), the SST is warmer in the western Pacific and its associated convection is stronger. In Figure 1b, AIRS detrended and deseasonalized CO<sub>2</sub> data for 17 La Niña months suggest that CO<sub>2</sub> has been lifted into the middle troposphere over the western Pacific. Lower mid-tropospheric CO<sub>2</sub> is seen in the eastern Pacific Ocean as a result of transport of low CO<sub>2</sub> from high altitude to the middle troposphere. Figure 1c presents the difference of mid-tropospheric CO<sub>2</sub> between El Niño and La Niña events. The difference, (El Niño - La Niña), of AIRS mid-tropospheric CO<sub>2</sub> is about 1–2 ppm over the central Pacific and –1 ppm over the western Pacific. This is consistent with changes in the Walker Circulation during El Niño and La Niña events. Student-t test is used to calculate the statistical significance of the difference for CO<sub>2</sub> concentration in El Niño and La Niña events. The CO<sub>2</sub> difference between El Niño and La Niña events are statistically significant when  $t$  is larger than a certain value  $t_0$ . The number of degrees of freedom for the CO<sub>2</sub> difference between two groups is 26. Given the number of degrees of freedom,  $t_0$  can be found from the  $t$  distribution table.  $t_0$  with a 5% significance level is 1.71. When the  $t$ -value plotted in Figure 1d is larger than 1.71, the results are within 5% significance level.

### 3.2. Impact of Polar Vortex on AIRS CO<sub>2</sub>

[13] The annular modes are the most dominant source of climate variability in the high latitudes. To investigate the influence of the northern hemispheric polar vortex on AIRS mid-tropospheric CO<sub>2</sub>, we averaged the detrended AIRS polar CO<sub>2</sub> north of 60°N from November to April, for the years 2003 through 2008. The result is shown as solid line in Figure 2a. The strength of the polar vortex is characterized by the northern annular mode (NAM) index, defined as the leading principal component time series of the sea-level pressure anomalies within November to April from 20°N to 90°N [Thompson and Wallace, 1998]. The detrended and inverted NAM index is shown as the dashed line in Figure 2a. Pearson's correlation coefficient for the detrended AIRS polar CO<sub>2</sub> and detrended inverted NAM index is 0.7, and the corresponding significance level is 9%. The significance statistics for correlations was generated by a Monte Carlo method [Press *et al.*, 1992; Jiang *et al.*, 2004]. Longer time series are needed to better understand the correlation between NAM and CO<sub>2</sub> concentration in the polar region.

[14] Figure 2a indicates that there are strong polar vortices in 2005 and 2007, i.e., for those years the NAM index is positive. Positive NAM is associated with a strong jet stream. It is hard for high concentrations of CO<sub>2</sub> outside to penetrate into the polar region. In addition, the increased

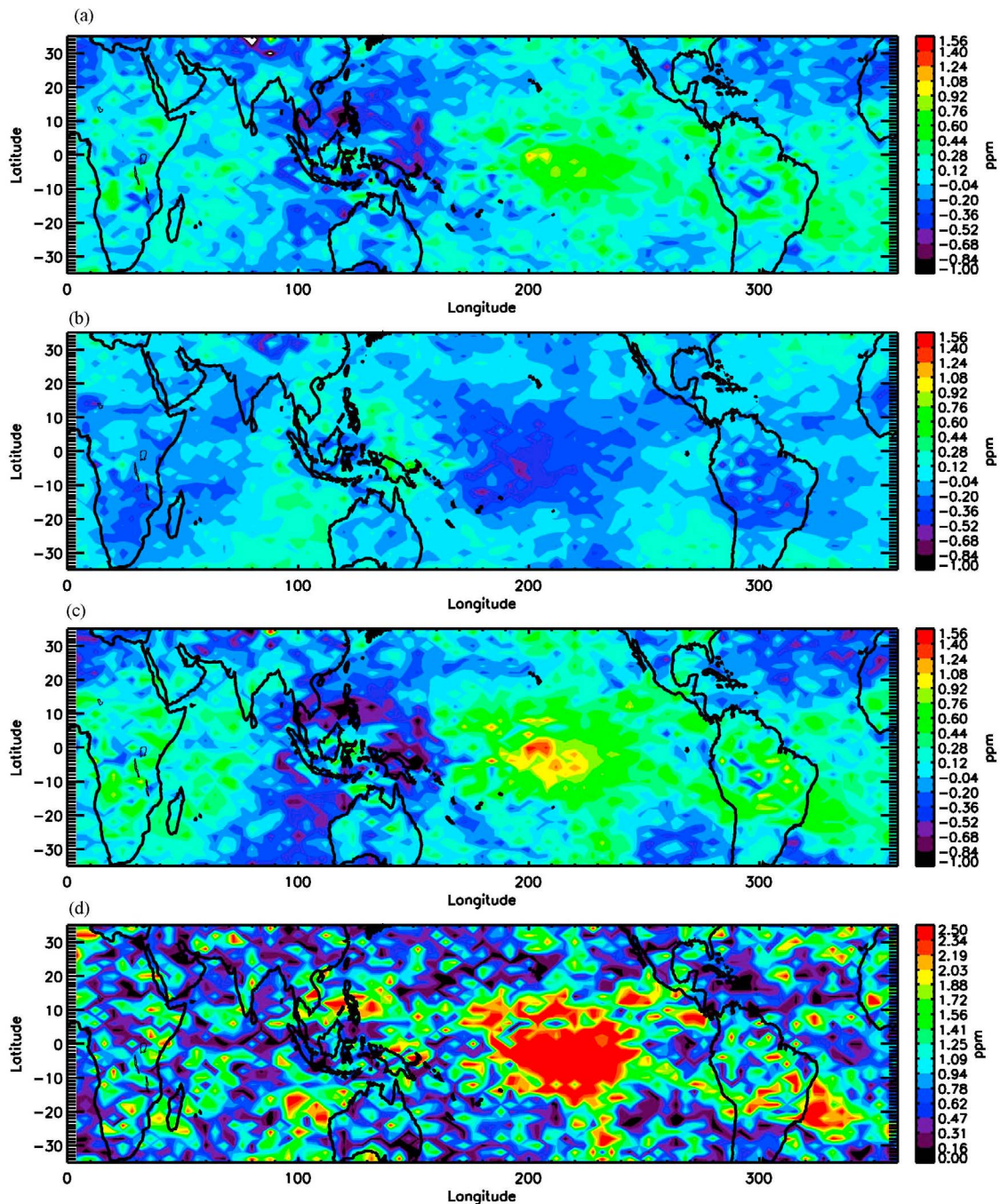


**Figure 1.** (a) AIRS detrended and deseasonalized CO<sub>2</sub> averaged for 11 El Niño months, (b) AIRS detrended and deseasonalized CO<sub>2</sub> averaged for 17 La Niña months, (c) AIRS CO<sub>2</sub> difference between El Niño and La Niña events, and (d) t-value for the CO<sub>2</sub> difference.

uptake of CO<sub>2</sub> by plants in spring [Russell and Wallace, 2004; Schaefer et al., 2005] might also contribute to the negative CO<sub>2</sub> anomalies in the strong polar vortex years. Figure 2b shows that the mean of AIRS detrended CO<sub>2</sub> from November to April in 2005 and 2007 was reduced in the polar region.

[15] On the other hand, Figure 2a indicates that the polar vortices are weak in 2006 and 2008. For the case of a weak polar vortex, it is easier for high concentrations of CO<sub>2</sub> outside to penetrate into the polar region. Figure 2c shows

that the AIRS detrended polar CO<sub>2</sub> was enhanced from November to April in 2006 and 2008. The difference of AIRS polar CO<sub>2</sub> between the strong polar vortex and weak polar vortex years is shown in Figure 2d. There is less CO<sub>2</sub> at the polar region for the strong polar vortex years. The absolute value of CO<sub>2</sub> difference between strong and weak polar vortices can reach 2–3 ppm. The number of degrees of freedom for the CO<sub>2</sub> difference between two groups is equal to 2. t-value with a 10% significance level is 2.9. When the



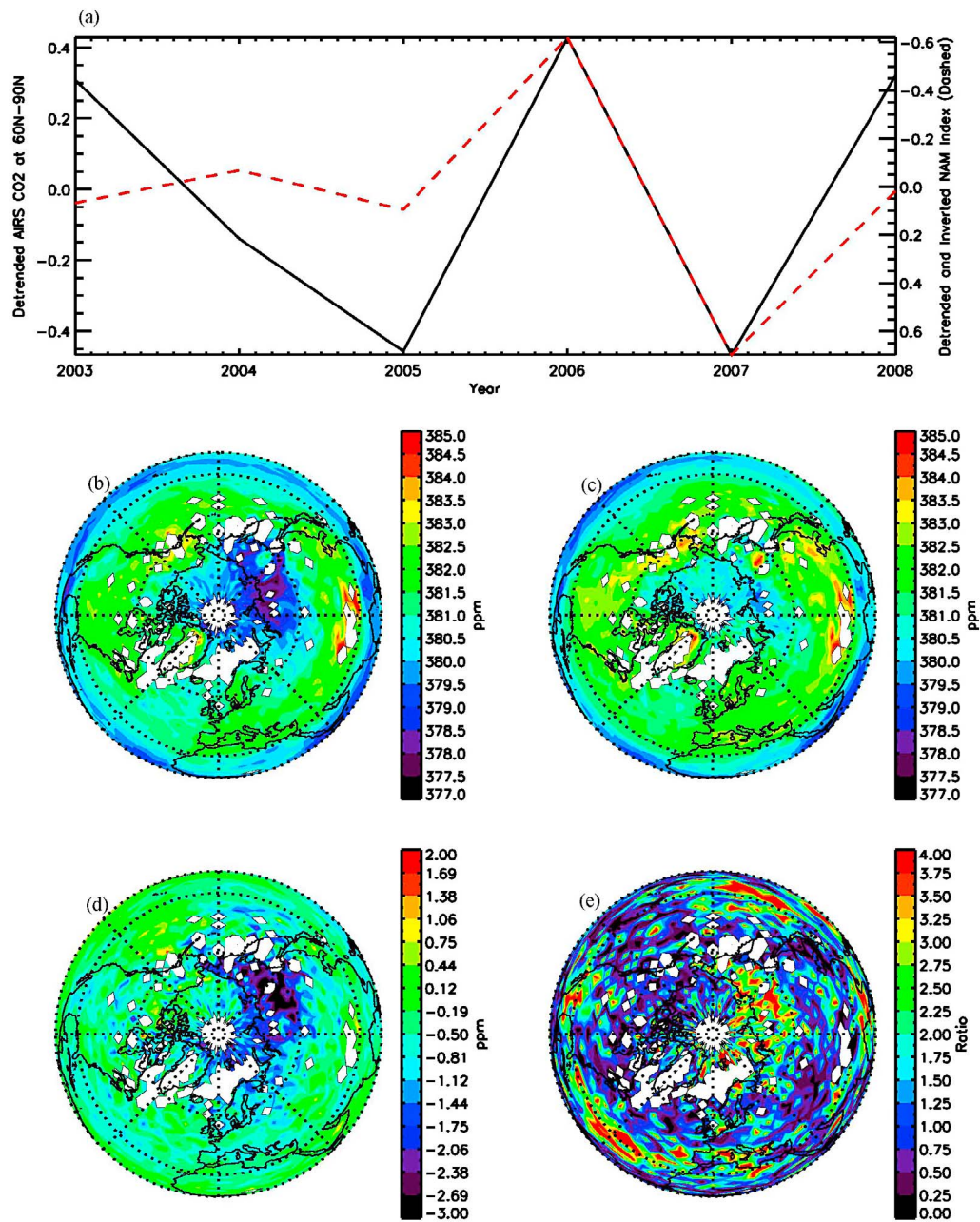


**Figure 2.** (a) AIRS detrended CO<sub>2</sub> (solid line) averaged from 60°N to 90°N and detrended NAM index (dash line, inverted). (b) AIRS detrended CO<sub>2</sub> average of 2005 and 2007, which are two strong polar vortex years. (c) AIRS detrended CO<sub>2</sub> averaged in 2006 and 2008, which are two weak polar vortex years. (d) Difference of AIRS CO<sub>2</sub> for strong and weak polar vortex years. (e) The t-value for the CO<sub>2</sub> difference. All CO<sub>2</sub> data are averaged from November to April.

t-value in Figure 2e is larger than 2.9, the results are within 10% significance level.

#### 4. Conclusions

[16] AIRS mid-tropospheric CO<sub>2</sub> retrievals have been used to investigate the interannual variability of CO<sub>2</sub> in the middle troposphere for the first time. Global CO<sub>2</sub> retrievals offer a unique opportunity to explore the relationships between the mid-tropospheric CO<sub>2</sub> concentration and large-

scale atmospheric processes. Our analysis suggests that the influences of El Niño events and polar vortex on the CO<sub>2</sub> concentration are apparent in the AIRS data. During El Niño, mid-tropospheric CO<sub>2</sub> is enhanced in central Pacific Ocean and diminished in the western Pacific Ocean. In the polar region, mid-tropospheric CO<sub>2</sub> is diminished if the polar vortex is strong. Polar mid-tropospheric CO<sub>2</sub> is enhanced if the polar vortex is weak. AIRS mid-tropospheric CO<sub>2</sub> increases our understanding of the interannual variabilities of atmospheric CO<sub>2</sub>. This analysis offers a unique oppor-

tunity for using chemistry-transport models to interpret the observations in more details in the future.

[17] **Acknowledgments.** This work was carried out at the Jet Propulsion Laboratory, California Institute of Technology, under contract with the National Aeronautics and Space Administration. X. Jiang is supported by JPL grant G99694. We thank two anonymous reviewers for helpful comments.

## References

- Aumann, H. H., et al. (2003), AIRS/AMSU/HSB on the Aqua mission: Design, science objectives, data products, and processing systems, *IEEE Trans. Geosci. Remote Sens.*, *41*, 253–264, doi:10.1109/TGRS.2002.808356.
- Bacastow, R. (1976), Modulation of atmospheric carbon dioxide by the Southern Oscillation, *Nature*, *261*, 116–118, doi:10.1038/261116a0.
- Bacastow, R., J. Adams, C. Keeling, D. Moss, T. Whorf, and C. Wong (1980), Atmospheric carbon dioxide, the Southern Oscillation, and the weak 1975 El Niño, *Science*, *210*, 66–68, doi:10.1126/science.210.4465.66.
- Chahine, M., C. Barnett, E. T. Olsen, L. Chen, and E. Maddy (2005), On the determination of atmospheric minor gases by the method of vanishing partial derivatives with application to CO<sub>2</sub>, *Geophys. Res. Lett.*, *32*, L22803, doi:10.1029/2005GL024165.
- Chahine, M. T., L. Chen, P. Dimotakis, X. Jiang, Q. Li, E. T. Olsen, T. Pagano, J. Randerson, and Y. L. Yung (2008), Satellite remote sounding of mid-tropospheric CO<sub>2</sub>, *Geophys. Res. Lett.*, *35*, L17807, doi:10.1029/2008GL035022.
- Dickinson, R. E., and R. J. Cicerone (1986), Future global warming from atmospheric trace gases, *Nature*, *319*, 109–115, doi:10.1038/319109a0.
- Feely, R. A., R. H. Gammon, B. A. Taft, P. E. Pullen, L. S. Waterman, T. J. Conway, J. F. Gendron, and D. P. Wisegarver (1987), Distribution of chemical tracers in the eastern equatorial Pacific during and after the 1982–1983 El Niño–Southern Oscillation event, *J. Geophys. Res.*, *92*, 6545–6558, doi:10.1029/JC092iC06p06545.
- Feely, R., et al. (1997), Variability of CO<sub>2</sub> distributions and sea-air fluxes in the central and eastern equatorial Pacific during the 1991–1994 El Niño, *Deep Sea Res., Part II*, *44*, 1851–1867, doi:10.1016/S0967-0645(97)00061-1.
- Feely, R. A., T. Takahashi, R. Wanninkhof, M. J. McPhaden, C. E. Cosca, S. C. Sutherland, and M.-E. Carr (2006), Decadal variability of the air-sea CO<sub>2</sub> fluxes in the equatorial Pacific Ocean, *J. Geophys. Res.*, *111*, C08S90, doi:10.1029/2005JC003129.
- Francey, R., et al. (1995), Changes in oceanic and terrestrial carbon uptake since 1982, *Nature*, *373*, 326–330, doi:10.1038/373326a0.
- Gage, K. S., and G. C. Reid (1987), Longitudinal variations in tropical tropopause properties in relation to tropical convection and El Niño–Southern Oscillation events, *J. Geophys. Res.*, *92*, 14,197–14,203, doi:10.1029/JC092iC13p14197.
- Inoue, H. Y., and Y. Sugimura (1992), Variations and distributions of CO<sub>2</sub> in and over the equatorial Pacific during the period from the 1986/88 El Niño event to the 1988/89 La Niña event, *Tellus, Ser. B*, *44*, 1–22, doi:10.1034/j.1600-0889.1992.00001.x.
- Jiang, X., C. D. Camp, R. Shia, D. Noone, C. Walker, and Y. Yung (2004), Quasi-biennial oscillation and quasi-biennial oscillation–annual beat in the tropical total column ozone: A two-dimensional model simulation, *J. Geophys. Res.*, *109*, D16305, doi:10.1029/2003JD004377.
- Jiang, X., S. Pawson, C. D. Camp, E. Nielsen, R. Shia, T. Liao, V. Limpasuvan, and Y. L. Yung (2008a), Interannual variability and trends in extratropical ozone. Part I: Northern Hemisphere, *J. Atmos. Sci.*, *65*, 3013–3029, doi:10.1175/2008JAS2665.1.
- Jiang, X., S. Pawson, C. D. Camp, E. Nielsen, R. Shia, T. Liao, V. Limpasuvan, and Y. L. Yung (2008b), Interannual variability and trends in extratropical ozone. Part II: Southern Hemisphere, *J. Atmos. Sci.*, *65*, 3030–3041, doi:10.1175/2008JAS2793.1.
- Jones, C. D., M. Collins, P. M. Cox, and S. A. Spall (2001), The carbon cycle response to ENSO: A coupled climate-carbon cycle model study, *J. Clim.*, *14*, 4113–4129, doi:10.1175/1520-0442(2001)014<4113:TCCRTE>2.0.CO;2.
- Keeling, C. D., T. P. Whorf, M. Wahlen, and J. Vanderpligt (1995), Interannual extremes in the rate of rise of atmospheric carbon dioxide since 1980, *Nature*, *375*, 666–670, doi:10.1038/375666a0.
- Meloen, J., et al. (2003), Stratosphere-troposphere exchange: A model and method intercomparison, *J. Geophys. Res.*, *108*(D12), 8526, doi:10.1029/2002JD002274.
- Press, W., S. Teukolsky, W. Vetterling, and B. Flannery (1992), *Numerical Recipes in FORTRAN 77: The Art of Scientific Computing*, 2nd ed., Cambridge Univ. Press, New York.
- Russell, J. L., and J. M. Wallace (2004), Annual carbon dioxide drawdown and the Northern Annular Mode, *Global Biogeochem. Cycles*, *18*, GB1012, doi:10.1029/2003GB002044.
- Schaefer, K., S. Denning, and O. Leonard (2005), The winter Arctic Oscillation, the timing of spring, and carbon fluxes in the Northern Hemisphere, *Global Biogeochem. Cycles*, *19*, GB3017, doi:10.1029/2004GB002336.
- Thompson, D. W. J., and J. M. Wallace (1998), The Arctic Oscillation signature in the wintertime geopotential height and temperature fields, *Geophys. Res. Lett.*, *25*, 1297–1300, doi:10.1029/98GL00950.
- Wong, C. S., et al. (1993), Changes in equatorial CO<sub>2</sub> flux and new production estimated from CO<sub>2</sub> and nutrient levels in Pacific surface waters during the 1986/87 El Niño, *Tellus, Ser. B*, *45*, 64–79, doi:10.1034/j.1600-0889.1993.00006.x.

M. T. Chahine, L. L. Chen, and E. T. Olsen, Science Division, Jet Propulsion Laboratory, California Institute of Technology, 4800 Oak Grove Dr., Pasadena, CA 91109, USA.

X. Jiang, Department of Earth and Atmospheric Sciences, University of Houston, 4800 Calhoun Rd., Houston, TX 77004, USA. (xjiang4@mail.uh.edu)

Y. L. Yung, Division of Geological and Planetary Sciences, California Institute of Technology, Mail Stop 150-21, Pasadena, CA 91125, USA.